ORIGINAL ARTICLE

Undifferentiated Human Adipose Tissue–Derived Stromal Cells Induce Mandibular Bone Healing in Rats

Claudio Parrilla, MD, PhD; Nathalie Saulnier, PhD; Camilla Bernardini, PhD; Riccardo Patti, MS; Tommaso Tartaglione, MD; Anna Rita Fetoni, MD, PhD; Enrico Pola, MD, PhD; Gaetano Paludetti, MD; Fabrizio Michetti, MD; Wanda Lattanzi, MD, PhD

Objective: To test the osteo-regenerative potential of adipose tissue–derived stromal cells (ATSCs), an attractive human source for tissue engineering, in a rat model of mandibular defect. Human dermal fibroblasts (HDFs) were used as a differentiated cellular control in the study.

Design: The ATSCs and HDFs were isolated from human lipoaspirate and skin biopsy specimens, respectively. Cells were characterized in vitro and then adsorbed on an osteo-conductive scaffold to be transplanted in a mandibular defect of immunosuppressed rats. Naked unseeded scaffold was used as a negative control.

Main Outcome Measures: Bone healing was studied by computerized tomography and histologic analysis after 4, 8, and 12 weeks.

Results: Computed tomography showed that undifferentiated ATSCs induced successful bone healing of the mandible defect when transplanted in animals, compared with HDFs and negative controls. Histologic analysis demonstrated that the newly formed tissue in the surgical defect retained the features of compact bone.

Conclusion: Undifferentiated human ATSCs are suitable for cell-based treatment of mandibular defects, even in the absence of previous osteogenic induction in vitro.

Arch Otolaryngol Head Neck Surg. 2011;137(5):463-470

Author Affiliations: Departments of Otolaryngology (Drs Parrilla, Fetoni, and Paludetti), Internal Medicine (Dr Saulnier), Radiology (Dr Tartaglione), Orthopaedics (Dr Pola), and Institute of Anatomy and Cell Biology (Drs Bernardini, Michetti, and Lattanzi and Mr Patti), Università Cattolica del Sacro Cuore, School of Medicine A. Gemelli, Rome, Italy; INSERM, Paris, France (Dr Saulnier); and Latium Muscular Skeletal Tissue Bank, Rome, Italy (Dr Michetti).

MANDIBULAR BONE DEfects, often resulting from trauma and demolitive surgery for tumoral diseases, represent a burden in otolaryngology clinical practice. Mandibular reconstruction is, in fact, usually hindered by the anatomical situation of the bone, which is prominent, lacks complete joint support, and is subjected to the muscular forces that can possibly distract the fracture site.[1] Current strategies for reconstructing bony defects are essentially based on 3 possible approaches: autograft bone, allograft bone, and artificial bone.[2,3] Autologous bone grafting still represents the gold standard because of its convenience, safety, therapeutic efficacy, and lack of immunity. Nevertheless, donor site morbidity issues and the complexity of surgical procedures affect the possible application of autografts in cases of large bone defects and increase the risk of surgical complications.[4]

Cell-based therapies for skeletal regeneration offer a paradigm shift that may provide alternative solutions. Ideal cells for skeletal regenerative medicine must be easily isolated without excessive morbidity, differentiate toward the osteogenic lineage, and maintain an adequate proliferative capacity after harvesting. Mesenchymal stromal cells, multipotent elements isolated from the stroma of adult and perinatal tissues, retain these characteristics. In particular, adipose tissue–derived stromal cells (ATSCs) exhibit extraordinary plasticity, being able to differentiate toward tissue lineages derived from the embryonic mesenchyme.[5-7] The osteogenic commitment of ATSCs on in vitro induction has been widely demonstrated in distinct experimental models.[8-12] However, the in vitro osteogenic differentiation process requires culturing for a long time along with non–clinically adaptable procedures, including cytotoxic treatments (eg, dexamethasone) or the use of gene transfer vectors, which are burdened with additional toxic effects and immunologic issues.[13,14]

In this study, we tested the osteogenic potential of human ATSCs that were neither differentiated nor engineered in vitro before transplantation, were adsorbed on a biomimetic osteoconductive scaffold, and were implanted in a rat model of critical size mandibular defect. Human dermal fibroblasts (HDFs), which could be considered a differentiated counterpart of mesenchymal stro-

mal cells, were used as cell controls in this study.[7] Previous studies[13,15] have approached the cell-based therapy of bone defects by focusing on different issues, such as the impact of different cell sources, scaffolds, growth factors, and gene transfer techniques for producing genetically modified cells. Local activation of distinct signaling cascades is required for fracture repair and bone regeneration.[16] Based on this rationale, the experimental hypothesis of this study was intended to verify the osteoinductive properties exerted by the dissected bone microenvironment on undifferentiated ATSCs implanted at the site of bone defect. For this purpose, a rat model of mandibular defect was chosen because previous studies[4,15] have demonstrated the pertinent use of such a model for the preclinical evaluation of alternative osteoinductive treatments.

METHODS

PATIENTS AND SPECIMENS

Adipose tissue–derived stromal cells were isolated from lipoaspirates of 3 patients aged 25 to 50 years from both sexes. Human dermal fibroblasts, which served as a "differentiated cell" control, were isolated from a 0.2-cm-diameter biopsy specimen of shaved skin obtained from the retroauricular region of healthy donors from both sexes aged 30 to 43 years. All the procedures used in this study were approved by the ethical committee of the Catholic University of Rome.

CELL ISOLATION, CULTURE, AND CHARACTERIZATION

Cell culture media, sera, and supplements were purchased from Lonza (Basel, Switzerland) unless otherwise specified. All the chemicals were purchased from Sigma-Aldrich Corp (St Louis, Missouri).

Adipose Tissue–Derived Stromal Cells

Adipose tissue specimens were extensively washed with a phosphate-buffered saline (PBS) solution and then were digested with 0.1% collagenase type VIII for 30 minutes at 37°C under gentle agitation. Enzymatic digestion was blocked by adding 10% fetal bovine serum, and the solution was filtered through 100-µm mesh to remove all residual tissue. The cell suspension was centrifuged at 200*g* for 5 minutes, and then pellet cells were seeded into a T75 tissue culture flask using Dulbecco modified Eagle medium supplemented with 10% fetal bovine serum and fibroblast growth factor β, 2 ng/mL. The next day, nonadherent cells were removed, and ATSCs were cultured up to 7 passages. The "mesenchymal" immunophenotype was confirmed by cytometry as previously described.[7]

Human Dermal Fibroblasts

Skin biopsy specimens were washed with a sterile PBS solution and then were mechanically mashed into small fragments. Each skin fragment was placed in a 35-mm culture dish and was incubated for 10 minutes at 37°C with 5% carbon dioxide and 85% humidity to increase the adhesion of the dermal surface to plastic. Complete culture medium (Dulbecco modified Eagle medium supplemented with 10% fetal bovine serum, 5% horse serum, penicillin [1 U/mL], and streptomycin [1 µg/mL]) was carefully added. Tissue cultures were incubated until confluent fibroblast layers were obtained; the tissue fragments were removed, and cells were expanded in T75 flasks.

The proliferation rate of both cell populations was measured using the trypan blue exclusion assay to compare the growth kinetics, as previously described.[7] The differentiation potential of both cell types was assessed to compare the plasticity of the 2 cell types before in vivo transplantation. Both ATSCs and HDFs were induced toward the osteogenic lineage in vitro as previously described.[10] Acquisition of the correct phenotype was analyzed morphologically using specific histologic staining, chemically by measuring the activity of alkaline phosphatase, and molecularly by analyzing the expression of osteospecific genes. The methods for the histologic and molecular procedures have been described elsewhere.[4,10] Alkaline phosphatase activity was evaluated in HDFs and ATSCs after 1, 2, and 3 weeks of osteogenic induction using cells cultured in growth medium as controls. The osteogenic medium was discarded, and cells were washed with PBS and then lysed with 1% Triton X-100 (Sigma-Aldrich Corp). The cell lysate was centrifuged at 14 000 rpm for 15 minutes at 4°C, and the supernatant was stored at –80°C for further analysis. Alkaline phosphatase activity was determined by measuring the conversion of p-nitrophenyl phosphate to p-nitrophenol using a commercially available kit (Olympus OSR6103; Olympus Life and Material Sciences, Hamburg, Germany) following the manufacturer's suggested procedures. The quantity of p-nitrophenol liberated from the substrate was determined by comparison with a standard curve. The absorbance was read at 405 nm using a microplate reader (Bio-Rad, Hercules, California). Enzyme activity was evaluated for 60 minutes and is expressed as maximum velocity. Reported values were normalized against the protein concentration determined in total cell lysate.

Animal Treatments

Undifferentiated ATSCs and HDFs were alternatively implanted into the mandibular bone defects created in recipient immunosuppressed rats to compare their bone regenerative capabilities in vivo.

Cell Preparation

To facilitate the delivery of cells, a nanocomposite osteoconductive scaffold composed of 20% hydroxyapatite and 80% collagen (HA/COL) was prepared and seeded with ATSCs and HDFs at the third culture passage suspended in sterile PBS, as previously described.[4] The distribution and viability of living cells adsorbed on the HA/COL composite have been demonstrated in a previous study[15]: enhanced green fluorescence protein–expressing fibroblasts adsorbed on the same scaffold were homogeneously seeded and expressed the transgene 1 month after implantation in the rat mandible.

Surgical Procedure

Twelve Wistar rats (250-300 g) were anesthetized via an intramuscular injection of ketamine hydrochloride (50 mg/kg) and xylazine (6 mg/kg). A 5 × 5-mm full-thickness defect was created in the mandible behind the root of the incisor, as described elsewhere.[4,15] The resulting defect was filled with the cell-scaffold compound, and the incisions were closed using polyglactin 910 (Vicryl; Ethicon Inc, Somerville, New Jersey). Six animals were treated with ATSCs, 6 received HDFs, and 6 received a mock treatment (a naked scaffold wetted with PBS solution) and served as controls. All the rats were immunosuppressed with daily subcutaneous administration of cyclosporine, 10 mg/kg/d, starting from the day of surgery and up to the tested time point. All the animals were fed a liquid diet during the first 4 weeks after surgery. Two animals per group

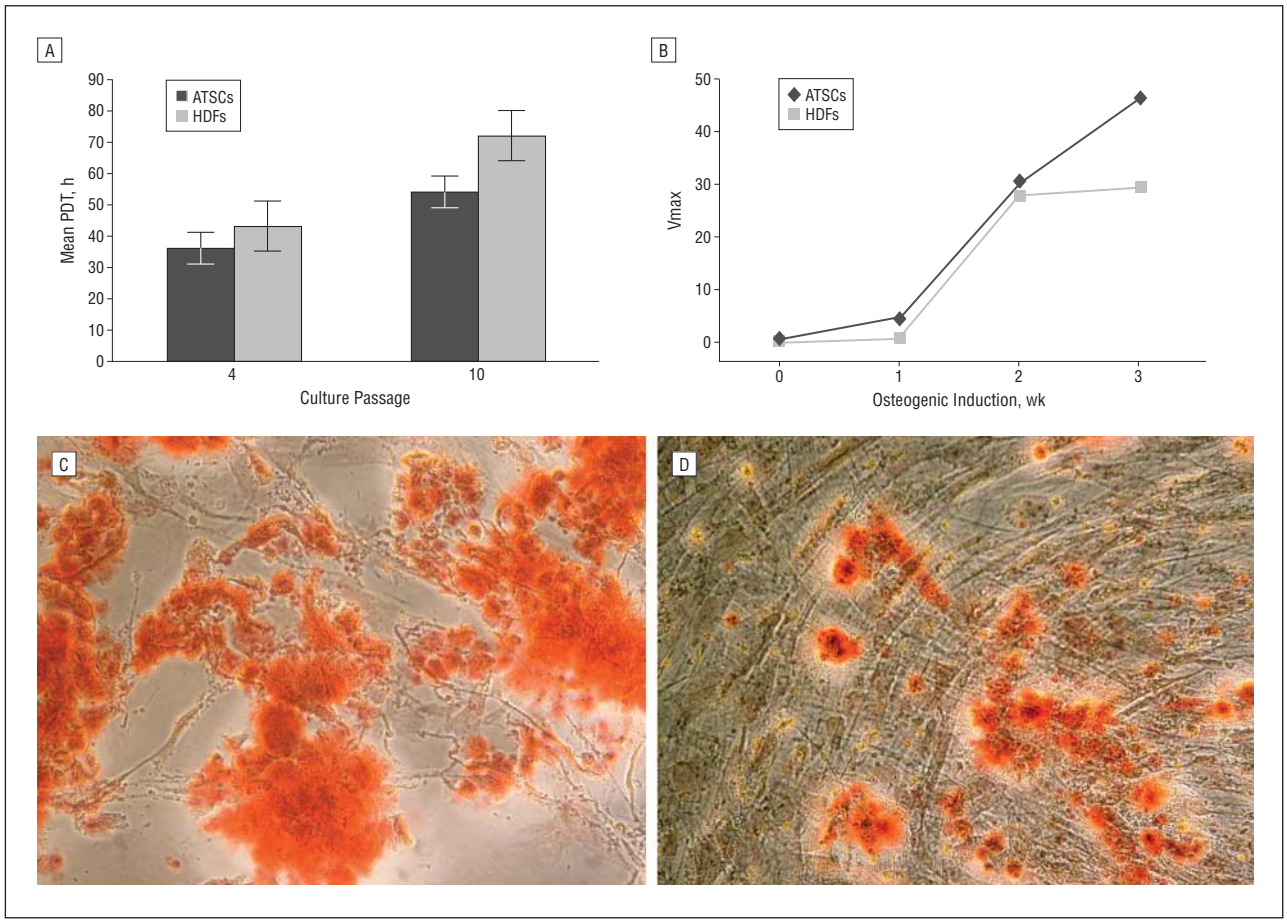

Figure 1. Cell growth and differentiation characteristics. A, Results of the trypan blue exclusion assay performed to measure the cell growth kinetics of the 2 cell types. Population doubling times (PDTs) of adipose tissue–derived stromal cells (ATSCs) and human dermal fibroblasts (HDFs) were calculated as means of replicate experiments based on the number of viable cells counted, as specified in the "Methods" section; a higher rate of cell duplication over time was observed for ATSCs than for HDFs at early culture passages, and at later culture passages, the differences in growth kinetics between the 2 cell populations were more evident. Error bars represent SD. B, Alkaline phosphatase–specific activity in ATSCs and HDFs during in vitro osteogenic differentiation. Enzymatic activity was statistically significantly increased after 2 weeks of culture under appropriate conditions. Data represent the mean (SEM) of 3 independent experiments ($P<.05$). Vmax indicates maximum velocity. Alizarin red staining of ATSCs and HDFs cultured for 3 weeks under osteoinductive conditions showed a higher increase in deposition of mineralized matrix in ATSCs (C) compared with in HDFs (D). Scale bars equal 10 μm.

were humanely killed 4, 8, and 12 weeks after the surgical procedures by lethal injection of pentobarbital sodium, 150 mg/kg intraperitoneally. Mandibular bone regeneration was assessed by computed tomography with tridimensional reconstruction (3D-CT). The extent of bone formation was measured in each animal by comparing the surface areas of the mandibular defect and of the bone tissue formed inside the defect based on the lateral view of 3D-CT images. Assuming the defect section to be approximately ellipsoidal, the horizontal and vertical diameters of the mandibular defect area were measured. The newly formed bone area was calculated by dividing the irregular-shaped surface into regular polygonal shapes. The surface areas of all the polygons in the area were then summed to obtain the total area of newly formed bone. Therefore, the "defect-filling" ratio was calculated as follows to obtain a percentage of bone defect filling: [newly formed bone area/(ellipsoidal defect area × 100)]. Defect-filling ratios were calculated in each animal to quantify the extent of newly formed bone. The rat mandibles were then processed for histologic analysis performed using hematoxylin-eosin staining, as previously described.[4,15]

All the animal-handling procedures and treatments were performed according to the guidelines for animal experimentation of the ethical committee of the Catholic University of Rome, which approved this study.

RESULTS

CELL CHARACTERISTICS

The characteristics of ATSCs and HDFs were analyzed in vitro before transplantation to clearly define their phenotypes. The growth characteristics of the 2 cell populations were quite different, as ATSCs showed a lower mean doubling time than did HDFs after 4 culture passages (**Figure 1**A). This divergence increased with culture passages, as HDFs progressively slowed down after the 15th passage. A drastic arrest in cell growth occurred after the 25th culture passage in ATSCs and the 20th in HDFs. These data agree with previous studies[7,17] demonstrating the higher proliferative rate of ATSCs compared with mesenchymal stromal cells isolated from different sources.

The osteogenic potential of ATSCs was confirmed after 3 weeks of in vitro osteogenic induction: the extent of the osteogenic differentiation of ATSCs and HDFs was confirmed by the increase in alkaline phosphatase activity after 1 week of culture in osteogenic medium (Figure 1B). Alizarin red staining confirmed a higher

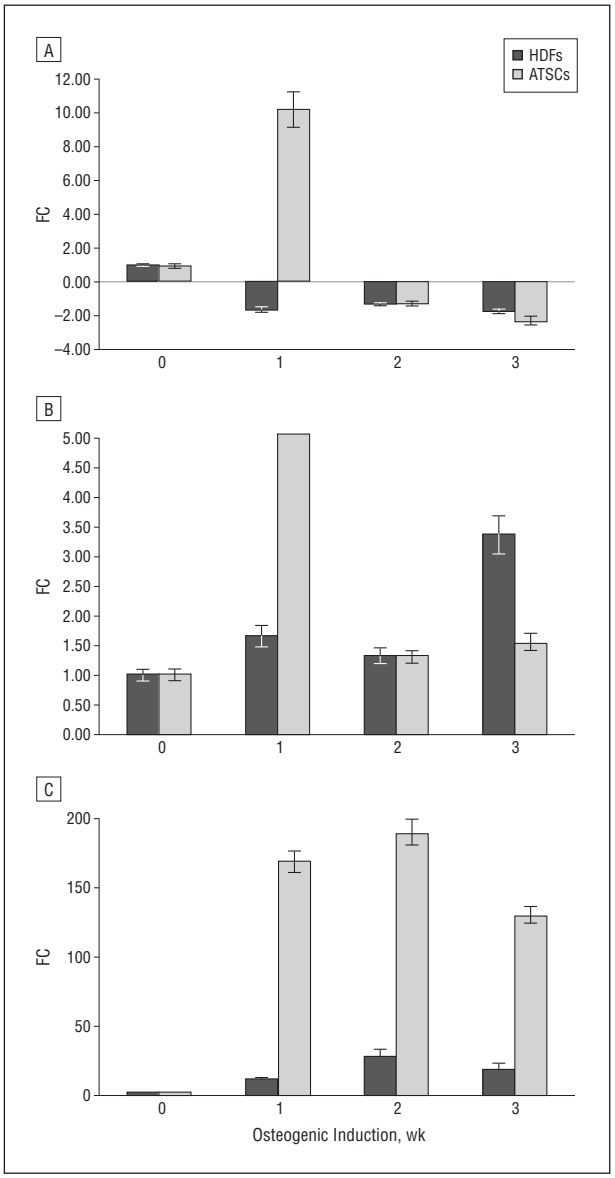

Figure 2. Gene expression analysis in adipose tissue–derived stromal cells (ATSCs) and human dermal fibroblasts (HDFs): *BMP2* (A), *RUNX2* (B), and *ALP* (C). Bone-related gene expression after 7, 14, and 21 days of in vitro culture in osteogenic medium. Differential expression is indicated as mean fold change (FC). Error bars represent SD. The FC was calculated using the ΔΔCt methods (see the "Methods" section for details).

osteogenic differentiation capacity in vitro of ATSCs (Figure 1C) compared with HDFs (Figure 1D). Finally, messenger RNA levels of bone-related genes were assessed by quantitative reverse transcription–polymerase chain reaction. Gene expression levels of the early osteogenic markers *RUNX2* and *BMP2* were transitorily increased in ATSCs at day 7 of in vitro culture with osteogenic medium; the expression of *RUNX2* underwent more than 3-fold upregulation in HDFs after 3 weeks of osteogenic induction. No significant change in either early gene was observed in HDFs at the first tested time points (**Figure 2**A and B). Expression of the late-stage osteogenic gene *ALP* was dramatically upregulated in both cell types after 1 week of induction and remained elevated during differentiation, with higher levels in ATSCs compared with in HDFs at all the tested time points (Figure 2C).

ANALYSIS OF BONE REGENERATION IN VIVO

A stable mandibular bone defect was created in all the rats without interrupting the bone continuity, as previously described.[4,15] The ATSCs and HDFs were alternatively adsorbed on the HA/COL osteoconductive scaffold and were implanted in a mandibular defect of recipient rats to comparatively evaluate their in vivo osteogenic potential. Rats treated with a naked scaffold served as negative controls. Both ATSCs and HDFs seeded on the HA/COL were vital and able to grow and proliferate 4 days after adsorption on the scaffold (data not shown). Moreover, a previous study[15] demonstrated that implanted cells were vital after the HA/COL–cell compound implantation in the rat mandible.

The chewing activity of rats treated with either ATSCs or HDFs was near normal as soon as 4 weeks after surgery, whereas control rats treated with a naked scaffold displayed a clear decrease in chewing ability at all the tested time points after surgery.

The occurrence of bone formation at the site of implantation was evaluated in 2 animals per group on humane killing 4, 8, and 12 weeks after surgery by 3D-CT and histologic analysis. None of the animals displayed evidence of systemic or local toxic effects related to either the implantation procedure or the immunosuppressive treatment. The entire mandible remained in its original position in all the rats, and fracture of the mandible arch occurred in 2 control animals, as described in the "Morphologic Analysis" subsection.

3D-CT ANALYSIS

The 3D-CT imaging revealed efficient repair of the mandibular defects implanted with ATSCs adsorbed on the HA/COL nanocomposite scaffold in a time-dependent manner compared with controls (**Figure 3**). To quantify the extent of new bone formation in the mandibular defect, a defect-filling ratio was calculated for each animal and is expressed as a percentage, as described in the "Methods" section (**Figure 4**). In particular, 26.6% (averaged defect-filling ratio between the 2 replicates) of the bone defect produced in the mandible was partially filled with newly mineralized tissue as soon as 4 weeks after the implantation of ATSCs (Figures 3A and 4). The amount of new bone increased up to 47.8% and 61.3% (average between replicates in each experimental group) 8 and 12 weeks after surgery, respectively (Figures 3B-D and 4). In rats treated with HDFs adsorbed on the scaffold, some extent of bone regeneration was observed, as the percentage of newly formed bone in the mandibular defect was below 17% up to 12 weeks after surgery (Figures 3E and F and 4). Nonsignificant amounts of new bone were observed in animals treated with HDF at the earlier time points (Figure 4). Modest and inefficient amounts of bone formation were observed in control animals treated with a naked HA/COL nanocomposite scaffold with sterile PBS. In particular, 2 control animals hu-

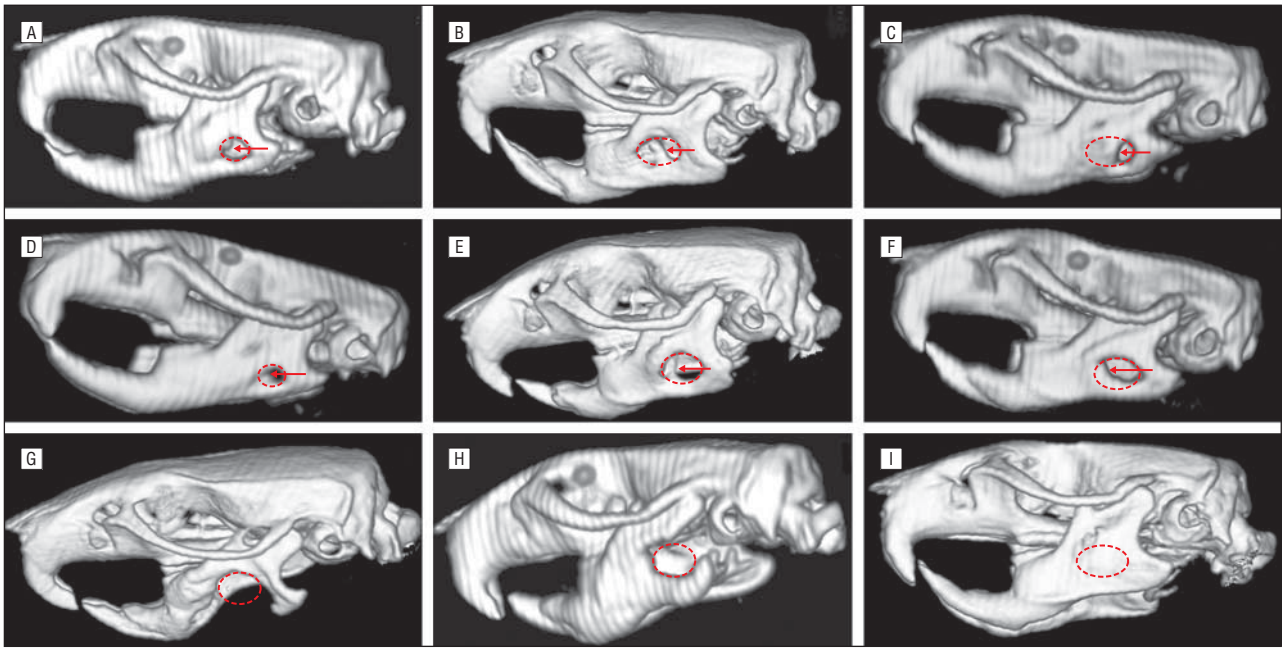

Figure 3. Computed tomography with tridimensional reconstruction analysis. The time-related bone regeneration process was observed in the defect created in the left mandible of rats treated with adipose tissue–derived stromal cells (ATSCs) and, to a lesser extent, of those treated with human dermal fibroblasts (HDFs). A, Rat treated with ATSCs at 4 weeks. B, Rat treated with ATSCs at 8 weeks. C and D, Rat treated with ATSCs at 12 weeks. E, Rat treated with HDFs at 8 weeks. F, Rat treated with HDFs at 12 weeks. G and H, Control rats at 12 and 8 weeks, respectively, with partial bone resorption of the mandible arch carrying the experimental defect. I, Entire healthy left mandible shown for reference. Dotted red circles indicate the defect size; red arrows point toward the borders of newly formed bone.

manely killed at 8 and 12 weeks showed a broken mandible branch as a result of partial bone resorption at the site of implantation (Figure 3G and H). In the remaining control animals, the mandible remained intact and the percentage of new bone surface in the surgical hole created in the mandible was 4% or less at all tested time points (Figure 4).

MORPHOLOGIC ANALYSIS

The morphologic features of the rat mandibles were then analyzed at the macroscopic and microscopic levels. The bone defect site was visible in both cell treatment groups as a smooth depression with a recognizable osseous callus in HDF- and ATSC-treated rats (**Figure 5**A and B). The mandibles of control animals treated with a naked scaffold allowed visualization of the full-thickness bone defect. The mandible arch was even fractured in 2 control rats (Figure 5C). Histologic analysis confirmed that the compact tissue formed in the defect displayed acidophilic affinity and uncontroversial aspects of mineralized compact bone (Figure 5D, E, G, H, J, and K). Particularly, in ATSC-treated mandibles, the newly formed bone tissue was evenly distributed, covering the defect size almost completely and reflecting the CT results. Connective tissue and traces of the reticular web of the HA/COL scaffold were visible in control mandibles (Figure 5F, I, and L).

COMMENT

Adipose tissue is commonly used for structural fat grafting in craniofacial and plastic surgery, where it has been proved to improve tissue regeneration rather than being simply a filler.[18] Although the biological mechanisms underlying the regenerative capabilities of adipose tissue are still unclear, a role of undifferentiated multipotent mesenchymal cells (ATSCs) in the stroma of fat grafts has been proposed.[18,19] In particular, ATSCs are known to efficiently differentiate toward the osteogenic lineage and increase bone regeneration on specific chemical induction or transfection with certain bone morphogenetic proteins.[8-12] Other researchers[10,20,21] have used ATSCs to induce bone healing in different animal models of cranial bone defects. These studies were based on cells induced toward the bone lineage in vitro using dexamethasone, which is known to exert systemic and local toxic effects, thus being inadequate for clinical application. Treatments with osteogenic factors or cell-transfection/transduction procedures are commonly used as alternative methods for ATSC differentiation for bone-healing purposes.[13,14] Although efficacious and effective, cell transduction and production of transgenic growth factors require non–clinically adaptable procedures. In particular, the use of either plasmid or viral vectors is burdened with toxic effects and immunologic issues that must be considered before translating such experimental procedures to the bedside.[4,14] The present study showed that human ATSCs, which were neither differentiated nor engineered before transplantation, implanted on a collagen-hydroxyapatite–based scaffold induced partial bone healing in an experimental model of rat mandibular defect. Although the bone defect was not completely healed, the bone regeneration allowed the functional recovery of treated rats. This finding could suggest that the microenvironment at the site of bone defect could induce the osteogenic commitment of ATSCs, promoting efficient bone healing in vivo. In fact, it has been demon-

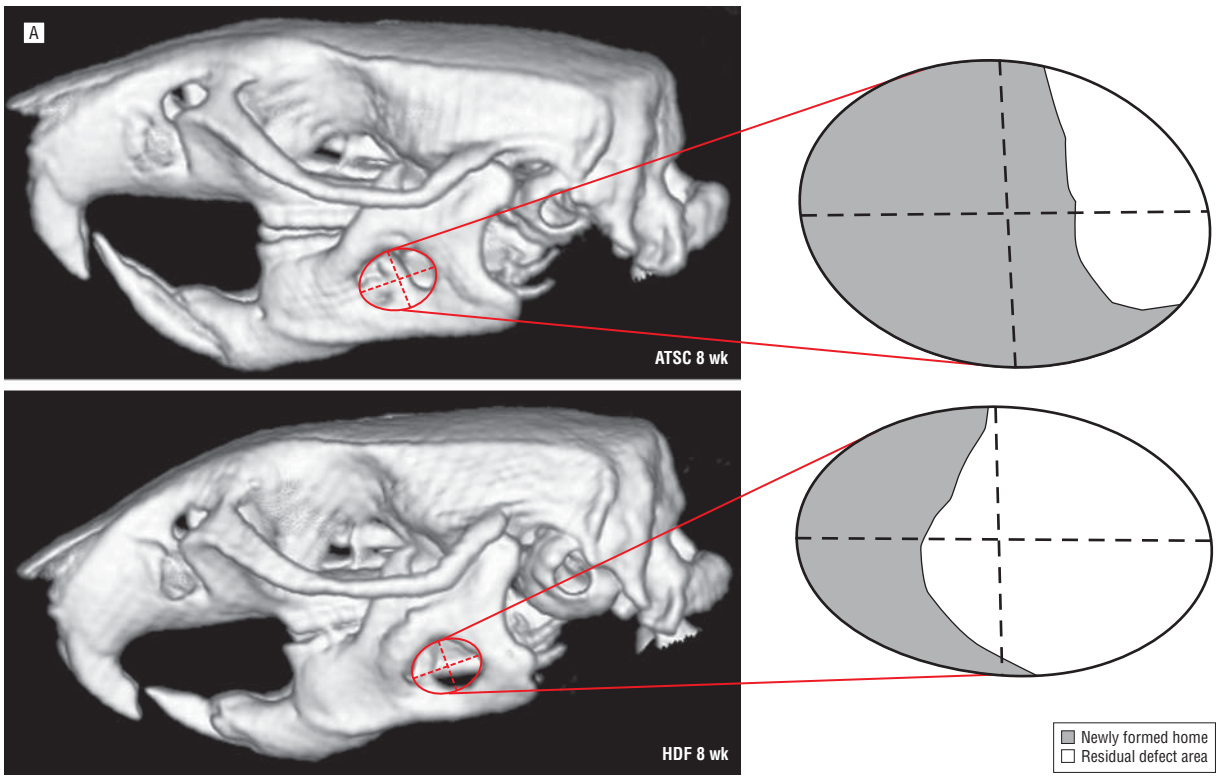

Treatment Group	Replicate No.	Tested Time Point, wk		
		4	8	12
ATSCs	1	33.02%	50.23%	63.45%
ATSCs	2	20.20%	45.48%	59.21%
HDFs	1	0.31%	29.42%	17.23%
HDFs	2	0.05%	5.33%	13.00%
CTRLs	1	2.32%	1.50%	NA
CTRLs	2	0.08%	NA	4.04%

Figure 4. Quantification of computed tomography results. The extent of bone healing was calculated in each rat as the ratio between the newly formed bone area and the ellipsoidal area of the mandibular bone defect obtained from the computed tomographic images. A, Representative graphical explanation of the area calculation procedure. B, Defect-filling ratios obtained from all the animals included in the treatment groups. ATSC indicates adipose tissue–derived stromal cell; CTRL, control; HDF, human dermal fibroblast; and NA, not assessed.

strated that during the early stages of bone healing, a variety of inflammatory cells infiltrate the injured site and stimulate the repair process. Interleukin 1β is required to promote the proliferation of osteoblasts and the production of mineralized bone matrix,[22] and bone morphogenetic proteins lead the molecular networking.[23] Inside the cell, wingless-type MMTV integration site signaling is a key player in promoting bone morphogenetic protein 2–mediated osteoblastic differentiation of mesenchymal progenitors during embryo development and bone healing.[24]

Therefore, in the experimental model described herein it could be hypothesized that the osteogenic commitment and subsequent differentiation of ATSCs in vivo occurred as a result of direct induction by locally produced growth factors and cytokines, which are physiologically implicated in the recruitment of local cells for new bone formation.[25] Further study to detect the expression profile of growth factors secreted at the site of bone defects could clarify this aspect.

We previously demonstrated that cells adsorbed on the HA/COL composite and implanted in the rat mandible were still viable and homogenously distributed on the weblike structure of the scaffold 1 month after surgery.[15] Together, these data could allow us to postulate that the implanted cells, rather than host surrounding cells, initiated the bone regeneration process. However, a significant contribution by the host mesenchymal stromal cells and preosteoblasts, proliferating at the site of bone defect and colonizing the scaffold, could not be excluded.

Some extent of bone regeneration was observed also in animals treated with HDFs compared with negative controls receiving a naked scaffold. Recent studies dem-

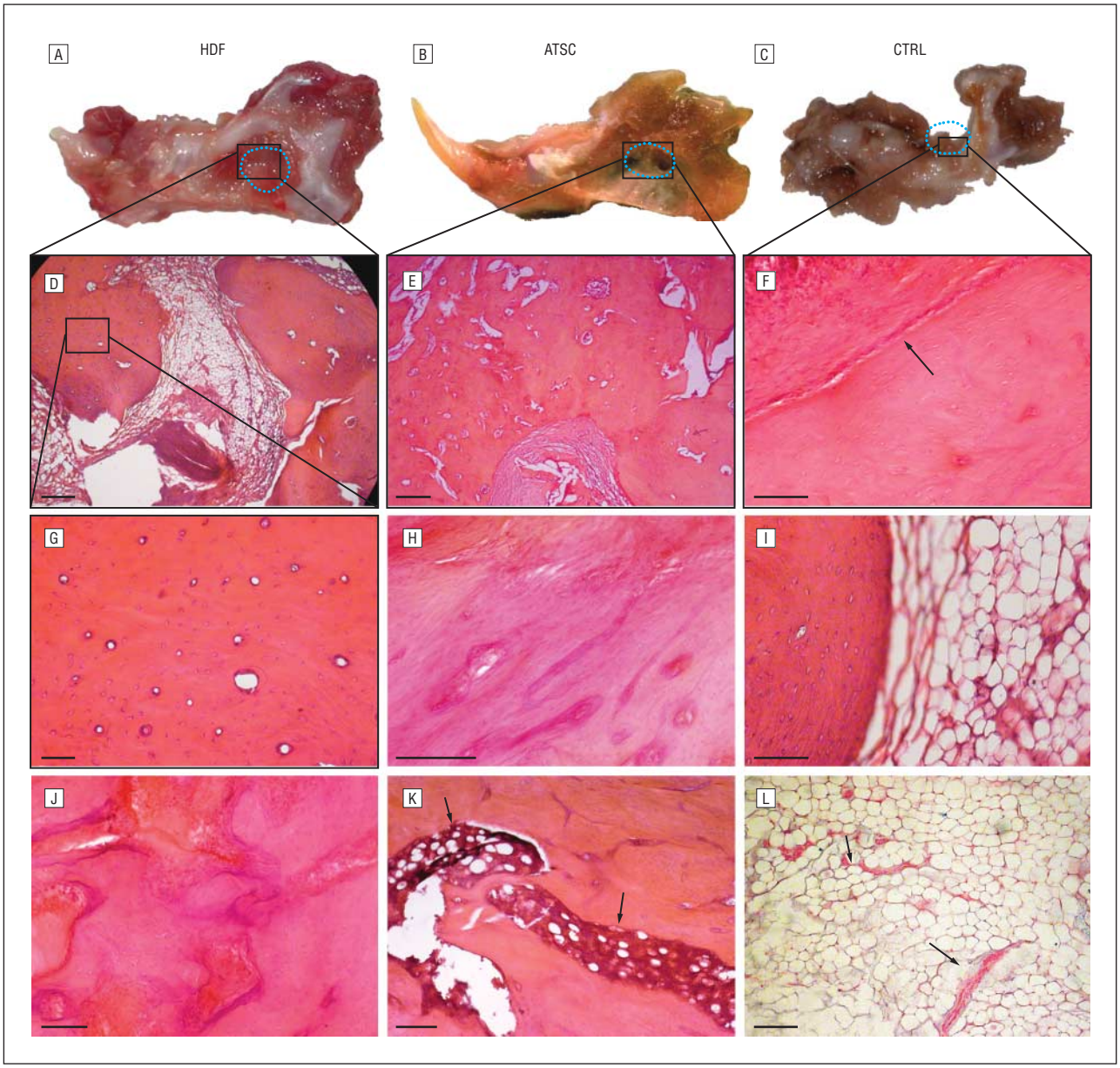

Figure 5. Histologic analysis. The rat mandibles were enucleated after humane killing to observe the mandibular defect site and then were decalcified and processed for histologic hematoxylin-eosin staining. The figures are representative of the morphologic appearance of the defect area in the 3 experimental groups at the macroscopic (A-C) and microscopic (D-L) levels. Dotted circles indicate the defect site, and squares are used to mark the microscopic field analyzed by histologic methods. A, In a human dermal fibroblast (HDF)–treated animal at 12 weeks, a smooth depression was visible on the bone surface at the site of the defect, with partial bone filling in the central area (arrow). B, In an adipose tissue–derived stromal cell (ATSC)–treated rat at 12 weeks, the defect appeared macroscopically as almost completely healed (mandible of the rat examined by computed tomography in Figure 3C). C, Mandible of a control (CTRL) rat at 8 weeks displaying the fracture of the area surrounding the full-thickness defect created in the arch. D, In an HDF-treated rat at 12 weeks, areas of compact bone tissue were surrounded by the connective matrix. Scale bar equals 0.5 mm. E, In an ATSC-treated mandible at 8 weeks, evenly distributed compact bone is visible as acidophilic tissue filling the mandibular defect. Scale bar equals 0.5 mm. F, In a CTRL animal treated with a naked 20% hydroxyapatite and 80% collagen scaffold at 12 weeks, connective scarlike tissue is visible along the border (arrow) of the bone defect. G, Higher magnification of the same microscopic field as in D showing compact bone structure with some haversian canals formed by the lamellar layers. Scale bar equals 100 µm. H, An ATSC-treated rat at 12 weeks. Scale bar equals 0.2 mm. I, In a CTRL mandible at 4 weeks, the microscopic structure of the scaffold is visible as an acidophilic reticular web (right side of the image). Scale bar=0.3 mm. J, An HDF-treated mandible at 12 weeks shows detail of the mineralized tissue formed at the defect site (distinct biological replicate from D and G). Scale bar equals 0.5 mm. K, An ATSC-treated rat at 4 weeks shows nonlamellar bone tissue with some traces of the scaffold (arrows) with cellular infiltrates. Scale bar equals 0.5 mm. L, In a CTRL mandible at 4 weeks, some cell infiltration and small vessels (arrows) are visible in the scaffold at higher magnification. Scale bar equals 100 µm.

onstrated the osteogenic capacities of genetically engineered dermal fibroblasts.[15,26-30] Also, a recent growing body of evidence confirms the idea of a certain degree of pluripotency potential in HDFs.[31-34] The diverse degree of new bone formation observed in animals treated alternatively with ATSCs and HDFs seemed to mirror the difference in cell osteogenic potentials analyzed in vitro (Figure 1B and C).

Conversely, implantation of a naked scaffold, in the absence of seeded cells, did not induce successful bone regeneration. This was expected considering that a stable nonunion defect model was used. Some aspects regarding the

effective role of grafted seeded cells in tissue regeneration are still controversial. Other authors described increased bone healing obtained through implantation of an unseeded scaffold in the presence of exogenous growth factors.[10,20,21] The osteogenic role of local autologous cells in the fractured site has been proposed to explain this finding, although this mechanism could be efficient only in cases of small bone defects. The experimental model used in this study represents a critical size defect, which is inherently more challenging in clinical practice. In this case, the use of an unseeded scaffold would not represent a valuable tool to induce efficient bone healing. Some authors observed that the amount of native cells from surrounding tissue might not be enough to efficiently generate bone tissue before degradation of the implanted scaffold.[35,36] This may result in scar tissue formation rather than bone formation at the site of the defect.[10]

Together, these data could encourage the development of innovative approaches based on the implantation of autologous undifferentiated stromal cells as alternative therapeutic strategies to be easily translated into clinical practice.

Submitted for Publication: June 21, 2010; final revision received November 29, 2010; accepted January 28, 2011.
Correspondence: Wanda Lattanzi, MD, PhD, Institute of Anatomy and Cell Biology, Università Cattolica del Sacro Cuore, School of Medicine, Largo F Vito 1, 00168 Rome, Italy (wanda.lattanzi@rm.unicatt.it).
Author Contributions: Drs Parrilla and Saulnier contributed equally to this study. All authors had full access to all the data in the study and take responsibility for the integrity of the data and the accuracy of the data analysis. *Study concept and design:* Paludetti and Lattanzi. *Acquisition of data:* Parrilla, Bernardini, Patti, Tartaglione, Pola, and Lattanzi. *Analysis and interpretation of data:* Parrilla, Saulnier, Fetoni, Michetti, and Lattanzi. *Drafting of the manuscript:* Parrilla, Bernardini, Patti, Fetoni, Michetti, and Lattanzi. *Critical revision of the manuscript for important intellectual content:* Saulnier, Tartaglione, Pola, and Paludetti. *Statistical analysis:* Parrilla, Saulnier, and Fetoni. *Obtained funding:* Paludetti. *Administrative, technical, and material support:* Parrilla, Saulnier, Patti, Tartaglione, and Fetoni. *Study supervision:* Paludetti, Michetti, and Lattanzi.
Financial Disclosure: None reported.
Funding/Support: This study was supported in part by the Università Cattolica del Sacro Cuore and the Latium Muscular Skeletal Tissue Bank.
Additional Contributions: Davide Bonvissuto, MLT, and Egidio Stigliano, MLT, provided technical assistance.

REFERENCES

1. Wong RC, Tideman H, Kin L, Merkx MA. Biomechanics of mandibular reconstruction: a review. *Int J Oral Maxillofac Surg*. 2010;39(4):313-319.
2. Wallace CG, Chang YM, Tsai CY, Wei FC. Harnessing the potential of the free fibula osteoseptocutaneous flap in mandible reconstruction. *Plast Reconstr Surg*. 2010;125(1):305-314.
3. Bak M, Jacobson AS, Buchbinder D, Urken ML. Contemporary reconstruction of the mandible. *Oral Oncol*. 2010;46(2):71-76.
4. Parrilla C, Lattanzi W, Rita Fetoni A, Bussu F, Pola E, Paludetti G. Ex vivo gene therapy using autologous dermal fibroblasts expressing hLMP3 for rat mandibular bone regeneration. *Head Neck*. 2010;32(3):310-318.
5. Zuk PA, Zhu M, Ashjian P, et al. Human adipose tissue is a source of multipotent stem cells. *Mol Biol Cell*. 2002;13(12):4279-4295.
6. Katz AJ, Tholpady A, Tholpady SS, Shang H, Ogle RC. Cell surface and transcriptional characterization of human adipose-derived adherent stromal (hADAS) cells. *Stem Cells*. 2005;23(3):412-423.
7. Saulnier N, Lattanzi W, Puglisi MA, et al. Mesenchymal stromal cells multipotency and plasticity: induction toward the hepatic lineage. *Eur Rev Med Pharmacol Sci*. 2009;13(suppl 1):71-78.
8. Cowan CM, Shi YY, Aalami OO, et al. Adipose-derived adult stromal cells heal critical-size mouse calvarial defects. *Nat Biotechnol*. 2004;22(5):560-567.
9. Hicok KC, Du Laney TV, Zhou YS, et al. Human adipose-derived adult stem cells produce osteoid in vivo. *Tissue Eng*. 2004;10(3-4):371-380.
10. Cui L, Liu B, Liu G, et al. Repair of cranial bone defects with adipose derived stem cells and coral scaffold in a canine model. *Biomaterials*. 2007;28(36):5477-5486.
11. Espitalier F, Vinatier C, Lerouxel E, et al. A comparison between bone reconstruction following the use of mesenchymal stem cells and total bone marrow in association with calcium phosphate scaffold in irradiated bone. *Biomaterials*. 2009; 30(5):763-769.
12. Zhao Y, Lin H, Zhang J, et al. Crosslinked three-dimensional demineralized bone matrix for the adipose-derived stromal cell proliferation and differentiation. *Tissue Eng Part A*. 2009;15(1):13-21.
13. Lattanzi W, Pola E, Pecorini G, Logroscino CA, Robbins PD. Gene therapy for in vivo bone formation: recent advances. *Eur Rev Med Pharmacol Sci*. 2005;9 (3):167-174.
14. Jeon O, Rhie JW, Kwon IK, Kim JH, Kim BS, Lee SH. In vivo bone formation following transplantation of human adipose-derived stromal cells that are not differentiated osteogenically. *Tissue Eng Part A*. 2008;14(8):1285-1294.
15. Lattanzi W, Parrilla C, Fetoni A, et al. Ex vivo-transduced autologous skin fibroblasts expressing human Lim mineralization protein-3 efficiently form new bone in animal models. *Gene Ther*. 2008;15(19):1330-1343.
16. Secreto FJ, Hoeppner LH, Westendorf JJ. Wnt signaling during fracture repair. *Curr Osteoporos Rep*. 2009;7(2):64-69.
17. Saulnier N, Puglisi MA, Lattanzi W, et al. Gene profiling of bone marrow- and adipose tissue-derived stromal cells: a key role of Kruppel-like factor 4 in cell fate regulation. *Cytotherapy*. 2011;13(3):329-340.
18. Coleman SR. Structural fat grafting: more than a permanent filler. *Plast Reconstr Surg*. 2006;118(3)(Suppl):108S-120S.
19. Clauser L, Polito J, Mandrioli S, Tieghi R, Denes SA, Galiè M. Structural fat grafting in complex reconstructive surgery. *J Craniofac Surg*. 2008;19(1):187-191.
20. Dudas JR, Marra KG, Cooper GM, et al. The osteogenic potential of adipose-derived stem cells for the repair of rabbit calvarial defects. *Ann Plast Surg*. 2006; 56(5):543-548.
21. Yuan J, Cui L, Zhang WJ, Liu W, Cao Y. Repair of canine mandibular bone defects with bone marrow stromal cells and porous β-tricalcium phosphate. *Biomaterials*. 2007;28(6):1005-1013.
22. Lange J, Sapozhnikova A, Lu C, et al. Action of IL-1β during fracture healing. *J Orthop Res*. 2010;28(6):778-784.
23. Kwong FN, Harris MB. Recent developments in the biology of fracture repair. *J Am Acad Orthop Surg*. 2008;16(11):619-625.
24. French DM, Kaul RJ, D'Souza AL, et al. WISP-1 is an osteoblastic regulator expressed during skeletal development and fracture repair. *Am J Pathol*. 2004; 165(3):855-867.
25. Frank O, Heim M, Jakob M, et al. Real-time quantitative RT-PCR analysis of human bone marrow stromal cells during osteogenic differentiation in vitro. *J Cell Biochem*. 2002;85(4):737-746.
26. Krebsbach PH, Gu K, Franceschi RT, Rutherford RB. Gene therapy-directed osteogenesis: BMP-7-transduced human fibroblasts form bone in vivo. *Hum Gene Ther*. 2000;11(8):1201-1210.
27. Nussenbaum B, Rutherford RB, Teknos TN, Dornfeld KJ, Krebsbach PH. Ex vivo gene therapy for skeletal regeneration in cranial defects compromised by postoperative radiotherapy. *Hum Gene Ther*. 2003;14(11):1107-1115.
28. Hirata K, Tsukazaki T, Kadowaki A, et al. Transplantation of skin fibroblasts expressing BMP-2 promotes bone repair more effectively than those expressing *Runx2*. *Bone*. 2003;32(5):502-512.
29. Phillips JE, Burns KL, Le Doux JM, Guldberg RE, García AJ. Engineering graded tissue interfaces. *Proc Natl Acad Sci U S A*. 2008;105(34):12170-12175.
30. Ishihara A, Zekas LJ, Litsky AS, Weisbrode SE, Bertone AL. Dermal fibroblast-mediated BMP2 therapy to accelerate bone healing in an equine osteotomy model. *J Orthop Res*. 2010;28(3):403-411.
31. Lysy PA, Smets F, Sibille C, Najimi M, Sokal EM. Human skin fibroblasts: from mesodermal to hepatocyte-like differentiation. *Hepatology*. 2007;46(5):1574-1585.
32. Junker JP, Sommar P, Skog M, Johnson H, Kratz G. Adipogenic, chondrogenic and osteogenic differentiation of clonally derived human dermal fibroblasts. *Cells Tissues Organs*. 2010;191(2):105-118.
33. Wernig M, Meissner A, Foreman R, et al. In vitro reprogramming of fibroblasts into a pluripotent ES-cell-like state. *Nature*. 2007;448(7151):318-324.
34. Lorenz K, Sicker M, Schmelzer E, et al. Multilineage differentiation potential of human dermal skin-derived fibroblasts. *Exp Dermatol*. 2008;17(11):925-932.
35. Kübler N, Michel C, Zöller J, Bill J, Mühling J, Reuther J. Repair of human skull defects using osteoinductive bone alloimplants. *J Craniomaxillofac Surg*. 1995; 23(6):337-346.
36. Clokie CM, Moghadam H, Jackson MT, Sandor GK. Closure of critical sized defects with allogenic and alloplastic bone substitutes. *J Craniofac Surg*. 2002; 13(1):111-123.